Fourier Consistency-based Motion Estimation in Rotational Angiography

Mathias Unberath[1,2], Martin Berger[1], André Aichert[1], Andreas Maier[1,2]

[1]Pattern Recognition Lab, Friedrich-Alexander-University Erlangen-Nuremberg
[2]Graduate School in Advanced Optical Technologies, Erlangen
mathias.unberath@fau.de

Abstract. Rotational coronary angiography allows for volumetric imaging but requires cardiac and respiratory motion management to achieve meaningful reconstructions. Novel respiratory motion compensation algorithms based on data consistency conditions are applied directly in projection domain and, therefore, overcome the need for uncompensated reconstructions.
Earlier, we combined single-frame background subtraction and epipolar consistency conditions to compensate for respiratory motion. In this paper, we show that background subtraction also enables motion estimation via optimization of novel Fourier consistency conditions.
The proposed method is evaluated in a numerical phantom study. Compared to the uncompensated case, we found a reduction in residual root-mean-square error of 89 % when Fourier consistency conditions were used. The results are promising and encourage experiments on clinical data.

1 Introduction

Providing physicians with models of the 3D anatomy of arterial trees is considered beneficial for diagnostic assessment and interventional guidance [1]. In the context of minimally invasive treatment of coronary artery disease, rotational angiography is an increasingly popular acquisition protocol that allows for 3D reconstruction of the vasculature [1,2].
Due to the low temporal resolution of clinical C-arm cone-beam CT (CBCT) scanners straight-forward 3D reconstruction is not always possible. Rotational angiography sequences are acquired over multiple seconds and, thereby, are corrupted by cardiac and respiratory motion. As a consequence, both motion patterns must be incorporated into reconstruction algorithms. Cardiac motion is high frequency and, as multiple recurrences are observed throughout the acquisition, is effectively handled by phase gating [1,2].
In contrast, respiratory motion is very low frequency and, consequently, quasi non-recurrent which imposes a need for intra-scan respiratory motion compensation. Most state-of-the-art methods rely on 3D-2D registration and assume that, albeit motion-induced inconsistencies prevail, meaningful initial reconstructions are possible [1]. This assumption, however, is a serious limitation to the applicability of aforementioned methods in presence of substantial motion.

To overcome this limitation, we recently proposed a motion compensation algorithm that operates directly in projection domain. The method is based on virtual single-frame material decomposition that enables motion estimation using data consistency conditions (CC) [3]. We employed epipolar CC [4] to assess the craniocaudal component of intra-scan respiratory motion [3]. In this work, we show that single-frame material decomposition also allows for the application of novel Fourier CC [5,6]. We compare the results obtained with both data consistency measures to a manually extracted ground-truth in a numerical phantom study based on XCAT [7].

2 Material and methods

We describe an algorithm for consistency-based motion assessment in rotational coronary angiography. First, non-truncated images of the contrasted lumen are obtained using virtual single-frame background subtraction. Second, novel Fourier consistency conditions are used to estimate detector domain shifts parallel to the rotation axis.

2.1 Virtual single-frame material decomposition

As the thorax extends beyond the 3D field of view of conventional C-arm CT scanners, rotational angiography acquisitions are truncated. Consequently, data consistency measures cannot be applied directly because scans exhibiting truncation are inherently inconsistent. While the thorax as a whole may be truncated, the contrast-filled coronary arteries only occupy the central volume and are, therefore, not truncated. We briefly restate the method proposed in [3] that allows for the single-frame separation of contrast agent and background in the sense of digital subtraction angiography.
Contrasted vessels manifest as small tubular structures that are bright with respect to the background. Filters enhancing these properties have been found effective for vessel segmentation. Here, we use a combination of morphological and Hessian-based filters to obtain a binary segmentation mask $\mathcal{W}_i$ of projection image $\mathcal{I}_i$, where $\mathcal{W}_i(\mathbf{u}) = 1$ if $\mathbf{u} \in \mathbb{R}^2$ belongs to the background and 0 otherwise. We seek to estimate a background image $\mathcal{B}_i$ that constitutes a non-contrast version of $\mathcal{I}_i$ to be used for digital subtraction. To this end, all evidence of contrast agent is removed from $\mathcal{I}_i$ yielding corrupted images $\mathcal{G}_i(\mathbf{u}) = \mathcal{I}_i(\mathbf{u}) \cdot \mathcal{W}_i(\mathbf{u}) \overset{!}{=} \mathcal{B}_i(\mathbf{u}) \cdot \mathcal{W}_i(\mathbf{u})$. Estimating $\mathcal{B}_i$ in spatial domain may lead to a patchy and unnatural appearance. Therefore, background estimation is performed in frequency domain by iterative deconvolution. Finally, the background estimate is subtracted from the contrasted projection, yielding a virtual digital subtraction angiogram $\mathcal{D}_i(\mathbf{u})$ that, ideally, only shows the contrasted vessels and is not truncated. Intermediate results of the pipeline are visualized in Figure 1.

(a) (b) (c) (d)

Fig. 1. Intermediate results and final digital subtraction angiogram of the numerical phantom data set. Figures 1(a) to 1(d) show the original projection, the segmentation mask, the background estimate, and the digital subtraction angiography image, respectively.

2.2 Fourier consistency

The background subtracted images $\mathcal{D}_i,\ i = 1, \ldots, M$ are not truncated and can be processed using data consistency conditions. Up to now, we employed consistency measures based on the epipolar geometry [4] to estimate detector domain shifts that optimize consistency.
However, consistency among projections cannot only be formulated in terms of epipolar geometry, but also in the Fourier domain of the sinogram. Edholm *et al.* [8] showed that there exist triangular regions in the Fourier transform (FT) of parallel-beam sinograms that have an absolute value close to zero, a property that enables the definition of Fourier Consistency Conditions (FCC). Recently, Berger *et al.* [6] proposed a heuristic extension of FCC for cone-beam geometries based on Brokish *et al.* [9].
The exact shape of the vacant regions depends on the acquisition geometry as well as the object's maximum extent r_p. For the fan-beam case it is given by

$$\left| \frac{\omega}{\omega - \xi \cdot D_{\text{SD}}} \right| > \frac{r_p}{D_{\text{SI}}}, \tag{1}$$

where D_{SD}, D_{SI} are the source-to-detector and source-to-isocenter distances, and ω, ξ are frequency variables associated with the projection angles and the detector rows, respectively. Let ψ be the frequency variable corresponding to the vertical detector direction. As changes in shape of the triangular regions at different ψ are negligible [9], Berger *et al.* proposed to extend the fan-beam condition stated in Equation 1 in the direction of ψ creating vacant regions for the 3D FT [6]. Similar to [3], we consider a motion model that consists of detector domain shifts in vertical direction that is parametrized by a sequence of shifts $\gamma = (\gamma_1, \ldots, \gamma_M)^\top$. The consistency metric that has to be optimized is given by

$$\text{FC}(\gamma) = \| \mathbf{W} \left(\mathbf{F} \cdot \mathbf{d}(\gamma) \right) \|_2^2 , \tag{2}$$

where $\mathbf{d}(\gamma) \in \mathbb{R}^K$ are the projection images $\mathcal{D}_i$ in vector format shifted according to γ, $\mathbf{F} \in \mathbb{C}^{K \times K}$ is a symmetric matrix that performs the 3D FT, and

Table 1. Root-mean-square error (RMSE) between the manually extracted shifts and the displacements obtained by optimization of Epipolar and Fourier CC, respectively. The results are stated in mm.

	Uncompensated	Epipolar CC	Fourier CC
RMSE	$(1.03 \pm 0.59) \cdot 10^1$	1.01 ± 0.83	1.11 ± 1.15

$\mathbf{W} \in \mathbb{R}^{K \times K}$ is a diagonal matrix that represents the 3D mask for the vacant regions. Moreover, $K = M \cdot U_1 \cdot U_2$, and $U_{1/2}$ is the size of the images $\mathcal{D}_i$ in $u_{1/2}$-direction, respectively. If the motion consists of projection domain shifts only as is the case here, the consistency metric defined in Equation 2 can be implemented very efficiently as the shifts can be applied in the 2D Fourier domain according to the shift theorem [5,6], yielding

$$\mathrm{FC}(\gamma) = \left\| \mathbf{W} \left(\mathbf{F}_i \left(\mathbf{T}(\gamma) \cdot \mathbf{F}_\mathbf{u} \cdot \mathbf{d} \right) \right) \right\|_2^2 . \tag{3}$$

$\mathbf{F}_i$ and $\mathbf{F}_\mathbf{u}$ are in $\mathbb{C}^{K \times K}$ and correspond to a 1D FT over the angles, and a 2D FT over the projections, respectively. The detector domain shifts along the u_2 direction are encoded as phase factors in $\mathbf{T}(\gamma) \in \mathbb{C}^{K \times K}$, such that

$$\begin{aligned} \mathbf{T}(\gamma) = \mathrm{diag}\Big(& \exp(-i2\pi\psi_1\gamma_1), \ldots, \exp(-i2\pi\psi_{U_2}\gamma_1), \\ & \exp(-i2\pi\psi_1\gamma_2), \ldots, \ldots, \exp(-i2\pi\psi_{U_2}\gamma_M) \Big) , \end{aligned} \tag{4}$$

where $\mathrm{diag}(\cdot)$ converts a vector to a matrix having the vector elements on the diagonal, and $\mathbf{d}$ is in row-major order. The derivative of Equation 4 with respect to γ_i can be computed analytically, allowing for an efficient gradient-based optimization of Fourier CC [6].

2.3 Experiments

We evaluate the proposed algorithm on a numerical thorax phantom based on XCAT, i.e. Cavarev [7]. The data set contains 128 projection images with 960×960 pixels with an isotropic pixel size of 0.308 mm. The acquisition is corrupted by substantial respiratory and cardiac motion, the respective surrogate signals are shown in Figure 2. Motion patterns are modeled such that no motion state is observed multiple times.

Projection images are processed according to Section 2.1 yielding non-truncated images of the contrasted lumen. Subsequently, detector domain shifts along the u_2-direction γ^{FCC} are estimated by optimization of Fourier consistency following Section 2.2. Moreover, we extract shifts that optimize epipolar CC γ^{ECC} following the method described in [3].

To enable quantitative evaluation, we manually tracked the position of two vessel bifurcation points over the acquisition, yielding a sequence of displacements. This step became necessary because, unfortunately, Cavarev does not include

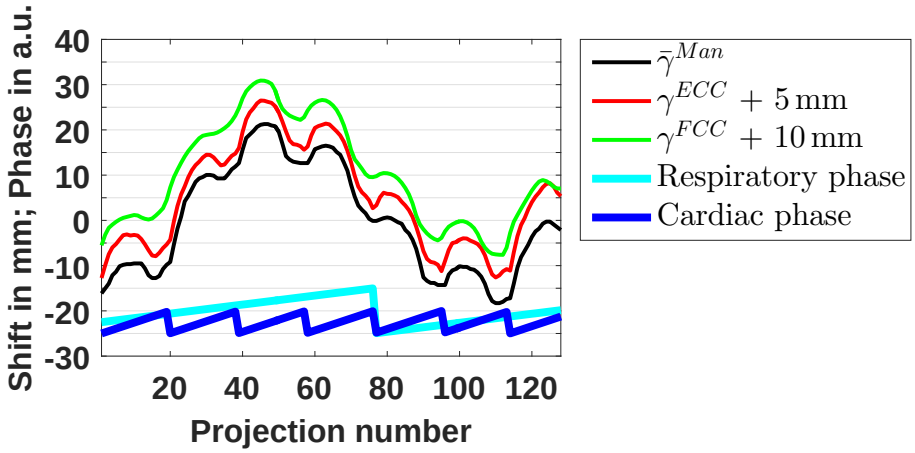

Fig. 2. We show shifts obtained by optimization of Fourier and Epipolar consistency, and the manually extracted ground-truth shifts. The motion patterns are slightly repositioned to avoid overlap and improve visualization: $\bar{\gamma}^{Man}$, γ^{ECC}, and γ^{ECC} are offset by 0, 5, and 10 mm, respectively. Normalized times indicating the respiratory and cardiac phase are shown at the bottom of the plot.

ground-truth motion patterns. For evaluation, we use the average displacement $\bar{\gamma}^{Man}$ and compute the root-mean-square error (RMSE) between $\bar{\gamma}^{Man}$ and the shifts extracted using Fourier and Epipolar CC, respectively.

3 Results

Shifts obtained by optimization of both data consistency measures are plotted in Figure 2 together with the respective motion phase that is stated using normalized time. It becomes apparent that all three motion patterns, namely $\bar{\gamma}^{Man}$, γ^{ECC}, and γ^{FCC} are very similar and exhibit global and local extrema at approximately the same positions. When considering the surrogate signals, one observes that the low frequency, high amplitude motion pattern correlates well with the respiratory phase. Moreover, local maxima occur around systole and suggest compensation of the craniocaudal displacement of the heart during contraction [3,10]. However, shifts estimated using Fourier CC exhibit less pronounced local extrema. This observation is also reflected in a higher RMSE that is stated in Table 1. While optimization of both consistency metrics resulted in RMSEs that are substantially lower than for the uncompensated case, the results obtained using epipolar CC are closer to the ground-truth.

4 Discussion

We showed that background subtracted rotational angiography images can be input to novel data consistency conditions based on Fourier properties of the

sinogram. We evaluated the proposed approach in a numerical phantom study on a XCAT-like phantom and obtained promising results. The shifts obtained by optimizing Fourier CC are in very good agreement with both, the ground-truth and the displacements obtained on the same data set with a method that optimizes epipolar consistency. Currently, consistency-based motion assessment in rotational angiography requires a sophisticated preprocessing pipeline to obtain an estimate of non-truncated images of the contrasted lumen. This requirement is a serious limitation for the applicability of consistency-based methods. Consequently, future work will investigate possibilities for less complex preprocessing. Finally, we plan to evaluate consistency-based motion assessment algorithms on real clinical data.

Acknowledgment

The authors gratefully acknowledge funding of DFG MA 4898/3-1 "Consistency Conditions for Artifact Reduction in Cone-beam CT", the Research Training Group 1773 "Heterogeneous Image Systems", and the Erlangen Graduate School in Advanced Optical Technologies (SAOT) by the German Research Foundation (DFG) in the framework of the German excellence initiative.

References

1. Çimen S, Gooya A, Grass M, Frangi AF. Reconstruction of Coronary Arteries from X-ray Angiography: A Review. Med Image Anal. 2016;32:46–68.
2. Unberath M, Achenbach S, Fahrig R, Maier A. Exhaustive Graph Cut-based Vasculature Reconstruction. In: Proc. ISBI. IEEE; 2016. p. 1143–1146.
3. Unberath M, Aichert A, Achenbach S, Maier A. Single-frame Subtraction Imaging. In: Proc. CT Meeting; 2016. p. 89–92.
4. Aichert A, Berger M, Wang J, Maass N, Doerfler A, Hornegger J, et al. Epipolar Consistency in Transmission Imaging. IEEE Trans Med Imaging. 2015;34(10):2205–2219.
5. Berger M, Maier A, Xia Y, Hornegger J, Fahrig R. Motion Compensated Fan-Beam CT by Enforcing Fourier Properties of the Sinogram. In: Proc. CT Meeting; 2014. p. 329–332.
6. Berger M. Motion-Corrected Reconstruction in Cone-Beam CT of Knees Under Weight-Bearing Conditions [Dissertation]. Friedrich-Alexander-University Erlangen-Nuremberg; 2016.
7. Rohkohl C, Lauritsch G, Keil A, Hornegger J. CAVAREV - An Open Platform for Evaluating 3D and 4D Cardiac Vasculature Reconstruction. Phys Med Biol. 2010;55(10):2905–2915.
8. Edholm PR, Lewitt RM, Lindholm B. Novel properties of the Fourier decomposition of the sinogram. In: Proc. SPIE 0671. International Society for Optics and Photonics; 1986. p. 8–18.
9. Brokish J, Bresler Y. Sampling requirements for circular cone beam tomography. In: Proc. NSS. vol. 5. IEEE; 2006. p. 2882–2884.
10. Shechter G, Resar JR, McVeigh ER. Displacement and Velocity of the Coronary Arteries: Cardiac and Respiratory Motion. IEEE Trans Med Imaging. 2006;25(3):369–75.